

TRPM2 channels are essential for regulation of cytokine production in lung interstitial macrophages

Sahasini Rajan  | Alexey Shalygin | Thomas Gudermann | Vladimir Chubanov | Alexander Dietrich 

Walther-Straub-Institute of Pharmacology and Toxicology, Member of the German Center for Lung Research (DZL), LMU-Munich, Munich, Germany

Correspondence

Alexander Dietrich, Walther-Straub-Institute of Pharmacology and Toxicology, Nußbaumstr. 26, 80336 Munich, Germany. Email: Alexander.Dietrich@lrz.uni-muenchen.de

Funding information

Deutsche Forschungsgemeinschaft; Deutsches Zentrum für Lungenforschung

Abstract

Interstitial macrophages (IMs) are essential for organ homeostasis, inflammation, and autonomous immune response in lung tissues, which are achieved through polarization to a pro-inflammatory M1 and an M2 state for tissue repair. Their remote parenchymal localization and low counts, however, are limiting factors for their isolation and molecular characterization of their specific role during tissue inflammation. We isolated viable murine IMs in sufficient quantities by coculturing them with stromal cells and analyzed mRNA expression patterns of transient receptor potential (TRP) channels in naïve and M1 polarized IMs after application of lipopolysaccharide (LPS) and interferon γ . M-RNAs for the second member of the melastatin family of TRP channels, TRPM2, were upregulated in the M1 state and functional channels were identified by their characteristic currents induced by ADP-ribose, its specific activator. Most interestingly, cytokine production and secretion of interleukin-1 α (IL-1 α), IL-6 and tumor necrosis factor- α in M1 polarized but TRPM2-deficient IMs was significantly enhanced compared to WT cells. Activation of TRPM2 channels by ADP-ribose (ADPR) released from mitochondria by ROS-produced H₂O₂ significantly increases plasma membrane depolarization, which inhibits production of reactive oxygen species by NADPH oxidases and reduces cytokine production and secretion in a negative feedback loop. Therefore, TRPM2 channels are essential for the regulation of cytokine production in M1-polarized murine IMs. Specific activation of these channels may promote an anti-inflammatory phenotype and prevent a harmful cytokine storm often observed in COVID-19 patients.

KEYWORDS

cytokine storm, IL-1 α , IL-6, reactive oxygen species (ROS), TNF- α , TRPM2 deficient mouse model

This is an open access article under the terms of the [Creative Commons Attribution](https://creativecommons.org/licenses/by/4.0/) License, which permits use, distribution and reproduction in any medium, provided the original work is properly cited.

© 2024 The Author(s). *Journal of Cellular Physiology* published by Wiley Periodicals LLC.

1 | INTRODUCTION

Our lungs are persistently exposed to pathogens from both sites: the airways and the vasculature. Next to dendritic cells and monocytes, resident macrophages are the most important for innate immune response in lung tissues and were initially differentiated from fetal monocytes or embryonic progenitor cells (Hoeffel et al., 2015; Sheng et al., 2015) reviewed in Gu et al. (2022). While in the airways alveolar macrophages (AMs) serve as a first line of defense, interstitial macrophages (IMs) act as gatekeepers of the vasculature and lung interstitium (see Aegerter et al., 2022; Cheng et al., 2021 for recent reviews). IMs were originally identified in preventing airway allergies like asthma in mice by producing interleukin-10 (IL-10), which has a dampening effect on dendritic cells in the lung (Bedoret et al., 2009). While AMs are easy to isolate from the broncho-alveolar lavage (BAL) fluid and are therefore already extensively studied, the exact roles and functions of IMs are currently unknown due to their remote parenchymal location and low cell counts. Up to three separable and substantially self-renewing populations of IMs were identified in the unchallenged “normal” lung (Gibbings et al., 2017). Although the exact roles of these IMs remain elusive, they exhibit different transcriptional profiles and were shown to be located in the interstitium of the bronchovascular bundles, but not in the alveolar walls (Gibbings et al., 2017). Murine IMs can be distinguished from AMs by the characteristic surface markers like CD11b and CX3CR1, their smaller size, and their irregular-shaped nuclei (reviewed in Gu et al., 2022). Next to their ability of self-renewal, which they share with AMs, IMs can be replenished by circulating monocytes (Gu et al., 2022). Like AMs, IMs form a pro-inflammatory M1 state, expressing tumor necrosis factor- α (TNF- α) and an M2 state for tissue repair, expressing arginase 1 (Arg1), after bacterial infection or an allergic challenge like ovalbumin (Dumigan et al., 2022; Ji et al., 2014; Nie et al., 2017; Peng et al., 2024; Strickland et al., 2023). Most interestingly, after introducing a more efficient way to isolate IMs (Ogawa et al., 2019), it was also possible to polarize isolated IMs in vitro to M1 or M2 states by adding lipopolysaccharide (LPS) and interferon- γ (IFN- γ) or IL-4, respectively (Tsurutani et al., 2021).

Transient receptor potential (TRP) channels are regulators of the intracellular Ca^{2+} concentration [Ca^{2+}]_i in many cells, including vascular smooth muscle, endothelial and immune cells (reviewed in Nilius & Szallasi, 2014). The second member of the TRP melastatin family (Chubanov et al., 2024) (TRPM2) forms tetrameric non-selective cation channels activated directly by ADP-ribose (ADPR) (Fliegert et al., 2017), but also by warm temperatures (Kamm et al., 2021; Song et al., 2016) among others generated during inflammation (Syed Mortadza et al., 2015). TRPM2 controls reactive oxygen species (ROS)-induced chemokine production in monocytes, which is responsible for the recruitment of inflammatory cells to the site of injury (Yamamoto et al., 2008). This channel also regulates inflammatory functions of neutrophils during infections with *Listeria monocytogenes* (Robledo-Avila et al., 2020) and, most interestingly, is also responsible for macrophage polarization and gastric inflammation during *Helicobacter pylori* infections (Beceiro et al., 2017).

Next to rather detrimental effects in these tissues, TRPM2 activation can also be beneficial and protects against tissue damage following oxidative stress (reviewed in (Maliougina & El Hiani, 2023; Miller & Cheung, 2016). As TRPM2 channels are also expressed in all three types of IM populations (see supplementary data in Gibbings et al., 2017), we set out to study their role in IM function. After establishing a protocol for the isolation of viable IMs, we identified characteristic currents induced by the TRPM2 activator ADPR. Importantly, TRPM2-deficient IMs polarized after application of LPS and IFN- γ produce and secrete a higher amount of IL-6, IL-1 α and TNF- α . TRPM2 activation induces membrane depolarization and less production of ROS resulting in a diminished cytokine secretion. Therefore, TRPM2 regulates cytokine production via a negative feedback loop to prevent massive cytokine secretion similar to a cytokine storm, often observed in COVID-19 patients.

2 | METHODS

2.1 | Animals

TRPM2-deficient (TRPM2^{-/-}) (Yamamoto et al., 2008) and wild-type mice from the same colony were used for all the experiments. All animal experiments were performed in accordance with the guidelines of the European Union for the use of animals.

2.2 | Isolation and propagation of interstitial macrophages and stromal cells

Briefly, the mice were killed by cervical dislocation. Bronchoalveolar lavage with cold phosphate buffer solution (PBS) was performed to remove alveolar macrophages. The thorax was exposed, and the lungs were flushed with warm HBSS by cardiac perfusion. Lungs were harvested, minced, and further subjected to enzymatic digestion with collagenase (4 mg/mL, C1-28; Sigma-Aldrich) in Dulbecco's modified Eagle's medium (DMEM) with no supplements for 50–60 min at 37°C stirred at 100 rpm. The digested lung tissue was homogenized with Pasteur pipette and cell suspension was filtered with 70 μM nylon filter (BD Falcon), followed by centrifuging at 4°C for 5 min at 300 rpm. The cell pellet was resuspended in DMEM (Lonza) supplemented with 10% fetal calf serum (FCS; Invitrogen), 1% penicillin/streptomycin (Lonza) and 50 mg/mL normocin (InvivoGen) and finally seeded in 10 cm cell culture dishes. The IMs were cocultured and propagated with stromal cells according to the method described by Ogawa et al. (2019) and Tsurutani et al. (2021) with some modifications. After 2 days, the supernatant was removed and the cells were washed with warm PBS to remove unattached cells like monocytes, erythrocytes. Treatment with 10 mM ethylene diamine tetra acetic acid (EDTA) in 10 mL DMEM for 20–30 min aided in detaching the cells. Cell suspension was centrifuged and the cells were split at 1:2 and plated with the medium being changed every 3–4 days. Cells were split again following the same method

after 6 days when over-confluent. AMs were isolated by centrifuging the broncho-alveolar lavage at 300 rpm at 4°C for 10 min and plating with Rosewell Park Memorial Institute (RPMI) 1640 medium with 10% FCS. The medium is removed after a day to remove unattached cells and the AMs were used for further analyses.

2.3 | Separation of stromal cells and interstitial macrophages

Cells in the second passage of coculture were detached with 10 mM EDTA after 6 days and centrifuged. The cell pellet suspended in the EasySep™ buffer (Stemcell Technologies; #20144) was subjected to immuno-magnetic separation using EasySep™ mouse CD11b positive selection kit II (Stemcell Technologies; #18970). Separated IMs were either directly used for flow cytometry, RNA isolation or seeded for in-vitro studies.

2.4 | RNA isolation and quantitative reverse transcription (qRT)–PCR analysis

Total RNA was isolated from IMs using RNeasy plus kit (Qiagen), from which first-strand cDNA was synthesized using RevertAid (Thermo Fischer Scientific). Real-time polymerase chain reaction (PCR) was performed using 2 × ABsolute™ QPCR SYBR Green Mix (Thermo Fischer Scientific). The reaction mixture contains 2 μL of cDNA from the first strand synthesis and 10 pmol of each primer pair (Table 1). PCR was carried out in a light-cycler (Roche) by adhering to the following steps: 15 min of initial activation followed by 45 cycles of 12 s at 94°C, 30 s at 50°C, and 30 s at 72°C. Fluorescence intensities were recorded after the extension step at 72°C after each cycle. Crossing points were determined by the software program provided by the manufacturer. Relative gene expression was quantified using the formula: $(2^{-(\text{Crossing point } \beta\text{-actin} - \text{Crossing point } X)}) \times 100 = \% \text{ of reference gene } (\beta\text{-actin}) \text{ expression.}$

2.5 | Flow cytometry

The expression of surface markers for IMs and AMs was detected in a flow cytometer (Guava easyCyte; Merck Millipore) using a cell density of $2 \times 10^5/\text{mL}$ in PBS containing 2% FCS and 0.5 mM EDTA. The cells were blocked with 0.5 μg of anti-mouse FcR (CD16/CD32, 553141; BD Biosciences) for 10 min RT to prevent nonspecific binding of the fluorochrome coupled antibody. The antibodies of interest (Table 2) were incubated for 20 min on ice and later washed twice with PBS to remove unbound antibodies. IMs were tested for macrophage-specific markers like CD11b–integrin αM, Mertk–myeloid epithelial reproductive tyrosine kinase, and Cx3cr1—a CX3C motif chemokine receptor 1. Another marker like MHCII—major histocompatibility complex II present in antigen-presenting cells was also tested. The M1 polarized IMs were examined for M1

TABLE 1 Primer pairs used for qRT-PCR.

Name	Sequence
TRPA1 forward	5'-TCTGCATATTGCCCTGCACA-3'
TRPA1 reverse	5'-TGGAAAATTTGGATCACTTCTTTGC-3'
TRPC1 forward	5'-GCCCCACCTTTCAACATTA-3'
TRPC1 reverse	5'-GTCGCATGGACGTCAGGTAG-3'
TRPC2 forward	5'-CACGAAAGGAGCCTGAGTTTA-3'
TRPC2 reverse	5'-CCAGCAACTCGAAGCCATAG-3'
TRPC3 forward	5'-AGGCGCAGCGTATGTGGA-3'
TRPC3 reverse	5'-GGCCAAAGCTCTCGTTTGC-3'
TRPC4 forward	5'-CTCCGCTGATCTCTGT-3'
TRPC4 reverse	5'-AAACGCGTTGTCTGTTTCT-3'
TRPC5 forward	5'-ATGAGGGGCTAACAGAAGA-3'
TRPC5 reverse	5'-TGCAGCTACATTGAAAGA-3'
TRPC6 forward	5'-CAAGCCTGTCTATTGAGGAA-3'
TRPC6 reverse	5'-CCCAACTCGAGACAAGTTT-3'
TRPC7 forward	5'-CCTACGCCAGGGATAAGTG-3'
TRPC7 reverse	5'-AAGGCCACAAATACCATGA-3'
TRPM2 forward	5'-TACCCACGAGCAACTT-3'
TRPM2 reverse	5'-GGAGACCCGGACATACTT-3'
TRPM7 forward	5'-GCAAAGCAGAGTGACCTGGTA-3'
TRPM7 reverse	5'-GCCAGTTGGCCAAATCAT-3'
TRPV2 forward	5'-CACCATAGTTGCCTACCACCA-3'
TRPV2 reverse	5'-GTCGCTTTGATGAGGGAAT-3'
TRPV3 forward	5'-CCACCACCATCTGGAACC-3'
TRPV3 reverse	5'-ATCTCCTGGAGTGGGCATT-3'
TRPV4 forward	5'-GATGGCCTTTCCGCTCTC-3'
TRPV4 reverse	5'-TCGGATGATGTGCTGAAAGA-3'
Mertk forward	5'-ACGTTGGTGATACGTGCAT-3'
Mertk reverse	5'-CTCTTCCCCTTCTCGGCAG-3'
Csf1 forward	5'-TACAAGTGAAGTGGAGGAGCCAT-3'
Csf1 reverse	5'-AGTCCTGTGTGCCAGCATAGAAT-3'
Csf1r forward	5'-AGGGCCATATACAGGTACACAT-3'
Csf1r reverse	5'-CACAGGCATCCATGTAACAC-3'
Csf2rb forward	5'-GGGCAGGAACACAGGACTTCAGGAC-3'
Csf2rb reverse	5'-CCAGGCCTTAGCTACCTTGACAGG-3'
CD11b forward	5'-ATGGACGCTGATGGCAATACC-3'
CD11b reverse	5'-TCCCCATTACGCTCTCCCA-3'
Cx3cr1 forward	5'-GAGTATGACGATTCTGCTGAGG-3'
Cx3cr1 reverse	5'-CAGACCGAACGTGAAGACGAG-3'
CD11c forward	5'-CTGGATAGCCTTTCTCTGCTG-3'

(Continues)

TABLE 1 (Continued)

Name	Sequence
CD11c reverse	5'-GCACACTGTGTCCGAAGTCA-3'
Socs3 forward	5'-CGAAGCACGCAGCCAGTT-3'
Socs3 reverse	5'-TCC GTG GGT GGC AAA GAA-3'
CD38 forward	5'-TCTCTAGGAAAGCCAGATCG-3'
CD38 reverse	5'-GTCCACACCAGGAGTGAGC-3'
CD86 forward	5'-CATGGGCTTGGCAATCCTTA-3'
CD86 reverse	5'-AAATGGGCACGGCAGATATG-3'
iNos forward	5'-GACATTACGACCCCTCCAC-3'
iNos reverse	5'-GCACATGCAAGGAAGGGAAC-3'
Nox1 forward	5'-GGTTGGGGCTGAACATTTTC-3'
Nox1 reverse	5'-TCGACACACAGGAATCAGGAT-3'
Nox2 forward	5'-TGTGGTTGGGGCTGAATGTC-3'
Nox2 reverse	5'-CTGAGAAAGGAGAGCAGATTCG-3'
Nox3 forward	5'-CAAGTGTGTGCTGTAGAGGAC-3'
Nox3 reverse	5'-CTATCCCGTAGCAACGAGTT-3'
Nox4 forward	5'-AGATTGCTGGAAGAACCCA-3'
Nox4 reverse	5'-GCTGCCATCGTTTCTGACAG-3'
β-Actin forward	5'-AAGGCAGTGGAGCAGGTGAA-3'
β-Actin reverse	5'-CCAGCAGACTCAATACACAC-3'

TABLE 2 Fluorochrome coupled antibodies for flow cytometry.

Antibody	Company	Clone	Conjugated fluorophore
CD11b	BioLegend	M1/70	FITC
Mertk	Thermo Fisher Scientific	DS5MMER	PE
CD38	BioLegend	90	FITC
MHCII	BioLegend	M5/114.15.2	APC/cyanine 7
Cx3cr1	BioLegend	SA011F11	PE
CD64	BioLegend	S18017D	PE
CD206 (MMR)	BioLegend	C068C2	FITC

marker CD38, a nicotinamide adenine dinucleotide (NAD⁺) hydrolase, which is specifically upregulated during inflammation in monocytes and macrophages (Li et al., 2022). Corresponding antibody isotypes were used for all antibodies as negative controls. Flow cytometry data were analyzed, and plots were created using R statistical software (packages—flowcore, ggcyto). Fluorescence intensities were quantified and represented as MFI—median fluorescence intensities.

2.6 | Polarization of IMs

IMs separated from WT and TRPM2^{-/-} stromal cells co-cultures were seeded at a density of 2.5×10^5 in 2 mL of DMEM with supplements in tissue culture treated six-well plates for RNA isolation and non-coated six-well plates for flow cytometry. Cells were allowed to attach for 16 h and subsequently stimulated to M1 polarization state by replacing medium with fresh medium containing 50 ng/mL lipopolysaccharide (LPS; Invitrogen) and 50 ng/mL IFN- γ (PeproTech) (Tsurutani et al., 2021). As a solvent control, 0.1% bovine serum albumin was added to the medium. For M2 polarization, IMs were treated with 20 ng/mL IL-4 (RnD systems). After 24 h of stimulation, cells were harvested for flow cytometry and RNA isolation.

2.7 | Quantification of cytokines by enzyme-linked immunosorbent assay (ELISA)

Supernatants were collected from WT and TRPM2^{-/-} IMs seeded for M1 and M2 polarization, described above, at 1, 3, 6, and 24 h and briefly centrifuged to remove dead cells. The supernatants were stored at -80°C . The concentrations of pro-inflammatory cytokines—tumor necrosis factor- α (TNF- α), IL-1 α , and IL-6 were detected using a murine Elisa max deluxe set (BioLegend; #430904, #433404, #431304, and #431414, respectively) according to the manufacturer's instructions. The assay diluent without cell supernatant was used as a blank. Finally, absorbance, which was read at 570 nm, was subtracted from the absorbance value at 450 nm. Four-parameter logistic curve-fitting for standards was performed and concentrations of cytokines in unknown samples were interpolated using GraphPad prism (version 10.1).

2.8 | Quantification of reactive oxygen species (ROS)

ROS were indirectly quantified in IMs treated with LPS and IFN- γ using a luminescence-based assay, GSH/GSSG-Glo assay (V6611; Promega), by measuring the levels of glutathione (GSH) and its oxidized form (GSSG) at 0, 10, 20, 30 and 40 min following treatment. The experiment was conducted according to the manufacturer's instructions. In addition, we quantified levels of ROS directly with the use of a fluorogenic probe 2',7'-dichlorodihydrofluorescein diacetate (H₂DCFDA, 10 μM , D399; Thermo Fischer Scientific), which emits fluorescence only when exposed to ROS. Briefly, 15,000 cells were seeded per well in a 96-well plate in DMEM (without phenol red) for 16 h before the procedure. Cells were treated with 10 μM H₂DCFDA for 60 min, followed by 15 min treatment with a selective inhibitor of NOX2 for (GSK2795039, 100 μM , SML2770; Merck). Finally, LPS and IFN- γ were added to cells at certain time points. Phorbol-12-myristat-13-acetate (PMA) (20 μM) was used as a positive control. In both experiments, the treatment was performed in HBSS without

serum. Luminescence for GSH/GSSG-Glo assay and fluorescence emitted by H₂DCFDA were detected using a microplate reader (Fluostar Omega; BMG Labtech).

2.9 | Electrophysiology

Patch-clamp experiments in the whole-cell configuration using voltage clamp or current clamp were performed with an EPC10 HEKA patch-clamp amplifier (Harvard Bioscience) and the PatchMaster software (Version V2x92; Harvard Bioscience) as reported previously (Mederos et al., 2008) with a few modifications. Patch pipettes were made of borosilicate glass (Science Products) and had a resistance of 2.0–3.7 MΩ when filled with the intracellular pipette solution. The extracellular solution contained in mM: 140 NaCl, 2.8 KCl, 1 CaCl₂, 2 MgCl₂, 10 HEPES-NaOH, and 11 glucose (all from Merck), pH 7.2. For whole-cell recordings of currents voltage ramps from -100 to +100 mV over 50 ms were applied every 2 s (holding potential between ramps was 0 mV). Voltages were corrected for a liquid junction potential of 10 mV. The current amplitudes at -80 and +80 mV were normalized to the cell size and presented as pA/pF. The capacitance was measured using the automated capacitance compensation function of the EPC10 software. Intracellular solution in mM: 140 Cs-glutamate, 8 NaCl, 1 MgCl₂, 10 HEPES-CsOH, pH 7.2, and in some experiments 0.2 ADPR (Merck) was applied. Current clamp experiments were performed with an intracellular solution, mM: 140 K glutamate, 8 NaCl, 1 MgCl₂, 10 Hepes-NaOH, pH 7.2, and 0.2 ADPR.

2.10 | Data mining and analysis

Transcriptome profile of murine IM by RNA sequencing was downloaded from the Gene Expression Omnibus RNA-seq database (GSE94135) and normalized counts of TRP channels were obtained using DESeq2 package in R statistical software. Statistical testing and data visualization were performed using GraphPad Prism version 10.1.2 (GraphPad Software). *T*-tests and one-way analysis of variance (ANOVA) were performed for flow cytometry experiments. Two-way ANOVA was performed for the detection of cytokines and oxidative stress. Wilcoxon matched pairs signed rank test was performed for data in Figure 5c. Paired *T*-test was used in Figure 7a. Data are shown as mean ± SEM, with significance denoted as asterisks indicating *p* < 0.05 (*), 0.01 (**), 0.001 (***) and 0.0001 (****).

3 | RESULTS

3.1 | Isolation of lung interstitial macrophages by propagation and magnetic separation

Usually, IMs are isolated by fluorescence-activated cell sorting (FACS) with a range of antibodies specific for IMs. A major disadvantage of

this method, however, is the very low cell count of IMs in steady state estimated to be ≈ 9% of extravascular myeloid cells, while it is ≈ 76% for AMs (Gibbings et al., 2017). In 2019, Ogawa et al. proposed an isolation method for resident macrophages not only from the lungs, but also from brain, spleen, and liver (Ogawa et al., 2019). Here, we present an improved version resulting in a higher number of isolated IMs (≈ 1.2 million cells per mouse compared to ≈ 30,000 cells per mouse after FACS isolation). After growth in a coculture with stromal cells, unstimulated IMs, which express the IM-specific CD11b protein (Gibbings et al., 2017), were isolated by immuno-magnetic separation using CD11b antibodies coupled to magnetic particles (Figure 1a). To validate this method, we characterized IMs for specific cell surface markers that differentiate them from AM by flow cytometry and qRT-PCR. Flow cytometric profiling revealed that IMs were positive for CD11b, Mertk, Cx3cr1, and CD64 (Figure 1b). IMs were mildly positive for MHCII, commonly expressed in antigen presenting cells and negative for CD206 (mannose membrane receptor), which is upregulated during anti-inflammatory conditions (Figure 1b). As a comparison, AMs were positive for Mertk and showed a low expression of CD64 and CD206, but were negative for CD11b, Cx3cr1, and MHCII (Figure 1c). By qRT-PCR experiments, high mRNA levels of CD11b, Cx3cr1, and colony stimulating factor 1 receptor (Csf1r) (Figure 1d) were detected in IMs. Csf1r, a surface protein majorly expressed in microglia (Lei et al., 2020), was recently found to be present in higher levels in IMs when compared to AMs (Meziani et al., 2018). MRNA levels of Mertk were clearly lower and mRNA for AM-specific colony-stimulating factor 2 receptor beta (Csf2rb) (Guilliams et al., 2013) was not detected in IMs (Figure 1d). The IMs isolated using our method, which were propagated with stromal cells and later separated, were therefore CD11b⁺ Cx3cr1⁺ Mertk⁺ MHCII^{lo} CD64⁺ CD206⁻ as already described before (Gu et al., 2022).

3.2 | Polarization of IMs

Most of the IMs isolated from unchallenged mice are in the unstimulated or naïve state and can be polarized after application of LPS and IFN-γ to the pro-inflammatory M1 state, while incubation with IL-4 results in differentiation to the anti-inflammatory M2 state (Tsurutani et al., 2021) (Figure 2a). We validated the polarization by quantification of mRNA levels for marker proteins specifically upregulated in M1 and M2 states. Along this line, mRNAs for inducible nitric oxide synthase (iNos/Nos2), suppressor of cytokine signaling 3 (Socs3), CD86 were highly expressed in the M1 states (Figure 2b–d), while arginase-1 (Arg-1) and resistin-like alpha (Retnlα) were upregulated in the M2 states (Figure 2f,g) (Gibbings et al., 2017), when compared to the unstimulated IMs. Recently, CD38 a surface glycoprotein, has gained more importance as a distinct M1 marker (Jablonski et al., 2015; Li et al., 2022). In bone-marrow-derived macrophages (BMDM), CD38 was expressed in higher quantities in M1 polarized macrophages. Like BMDM, M1 polarized IMs expressed higher levels of CD38 mRNAs (Figure 2e) and were also positive for CD38 protein compared to naïve and M2 polarized IMs (Supporting

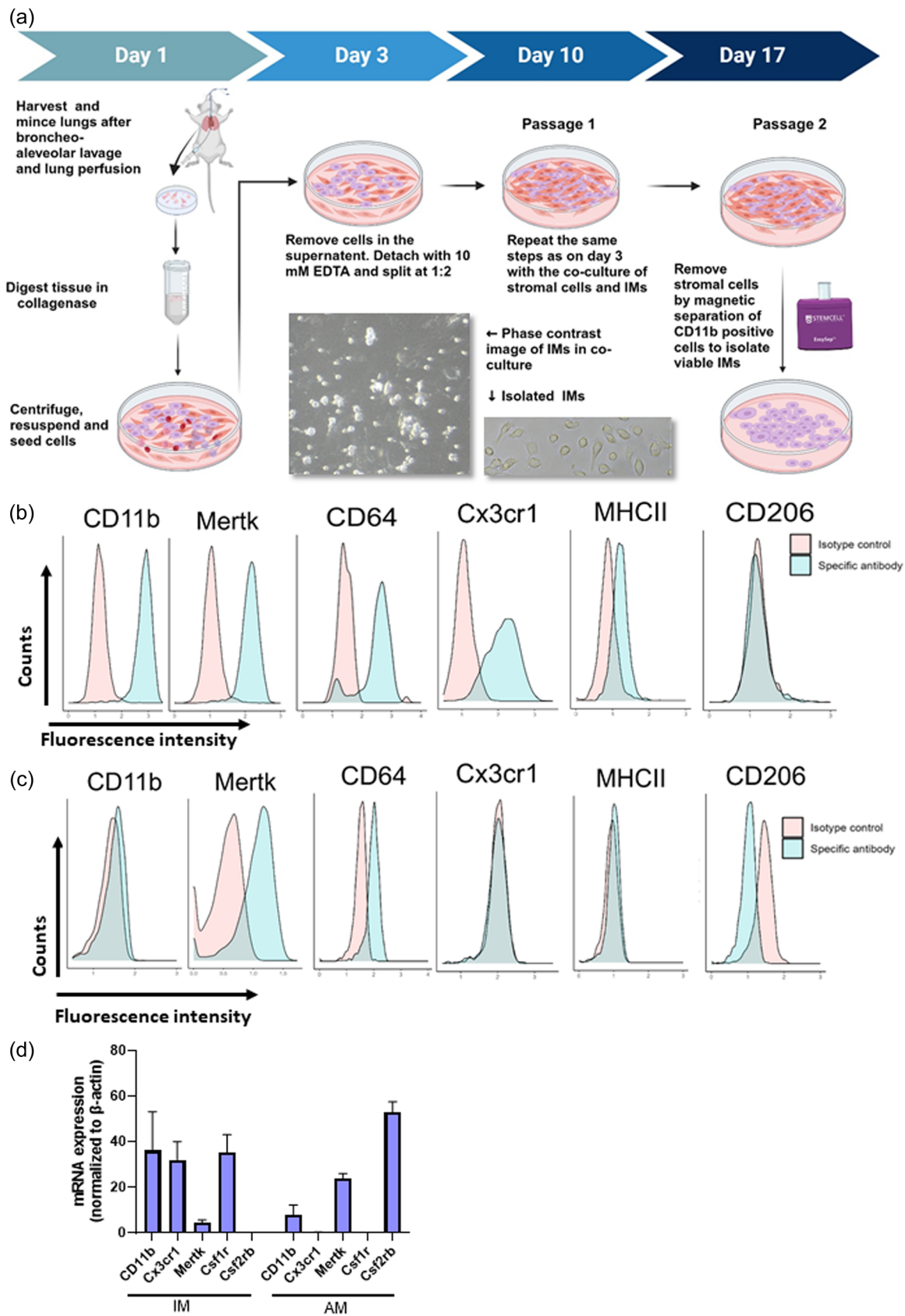


FIGURE 1 (See caption on next page).

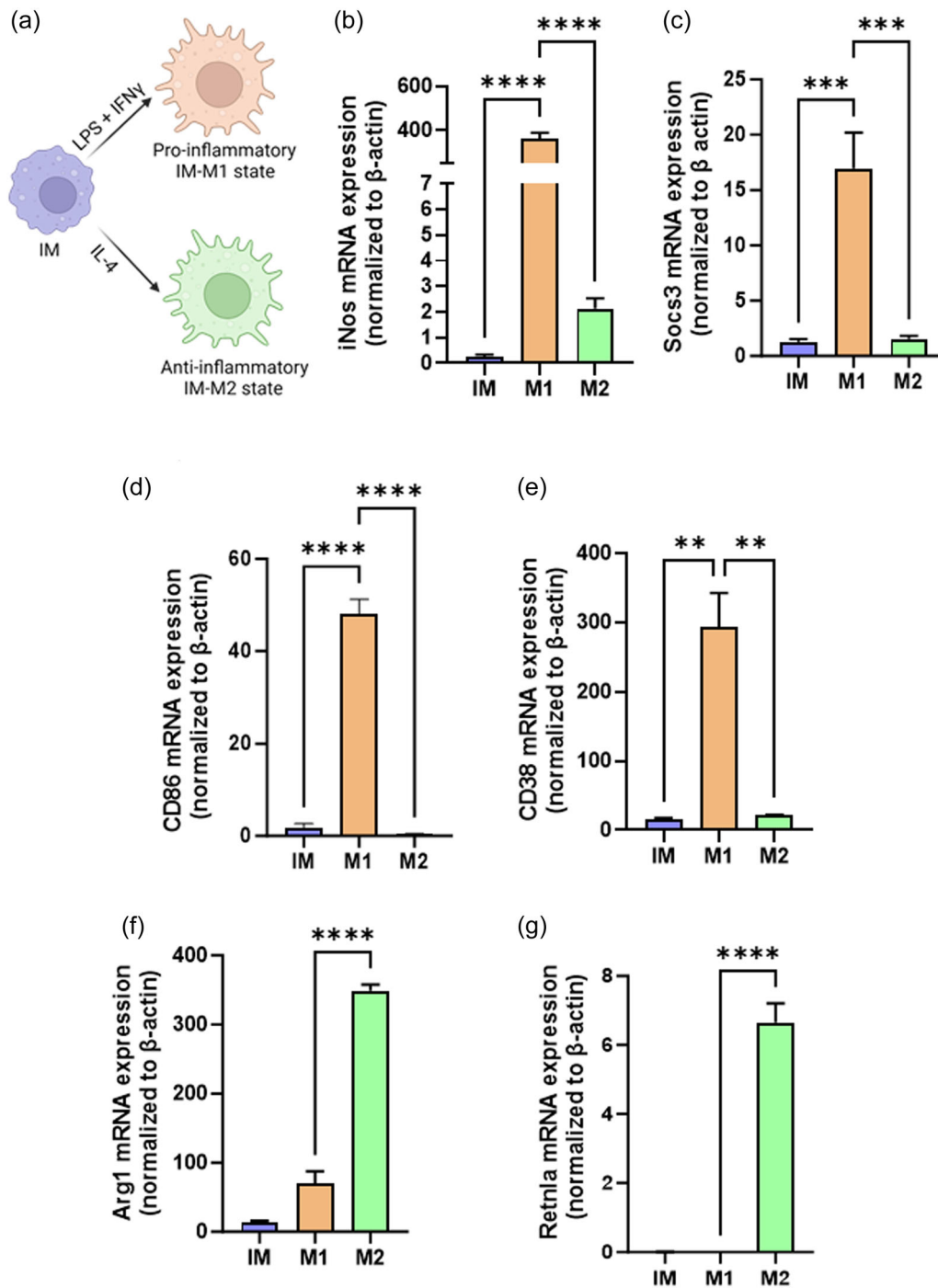


FIGURE 2 IM polarization. (a) Schema of the polarization protocol to obtain IM-M1 state and IM-M2 state cells from unstimulated IMs (IM). MRNA levels of M1-specific marker proteins iNos (b), Socs3 (c), CD86 (d) and CD38 (e) as well as M2-specific marker proteins Arg1 (f) and Retnla (g) in unstimulated IMs, IMs polarized to the M1 state (M1), and IMs polarized to the M2 state (M2). All samples are normalized to the expression of the housekeeping gene β -actin. $n = 3$ samples per group, ** $p < 0.01$, *** $p < 0.001$, **** $p < 0.0001$.

FIGURE 1 Isolation and characterization of IMs from murine lungs. (a) Timeline for isolation of IMs utilizing a coculture with stromal cells and magnetic separation of CD11b positive cells. (b, c) Representative histograms ($n = 3-6$ cell isolations) obtained by application of specific antibodies (in blue) or its corresponding isotype controls (in pink) from flow cytometric analyses of isolated IMs (b) and AMs as control cells (c). (b) Histograms of isolated IMs obtained after application of antibodies directed against typical marker proteins (CD11b, Mertk, CD64, Cx3cr1, MHCII and C206). MHCII is lowly and CD206 is not expressed at the plasma membrane of murine IMs. (c) Histograms of isolated AMs obtained after application of antibodies directed against typical marker proteins (CD11b, Mertk, CD64, Cx3cr1, MHCII, and C206). CD11b, Cx3cr1, and MHCII are not expressed in AMs. (d) mRNA levels of IM-specific marker proteins CD11b, Cx3cr1, and colony-stimulating factor 1 receptor (Csf1r), a general macrophage marker, Mertk, and the AM-specific marker protein (Csf2rb) detected by quantitative RT-PCR in the isolated IMs and AMs. $n = 3-5$ samples per group.

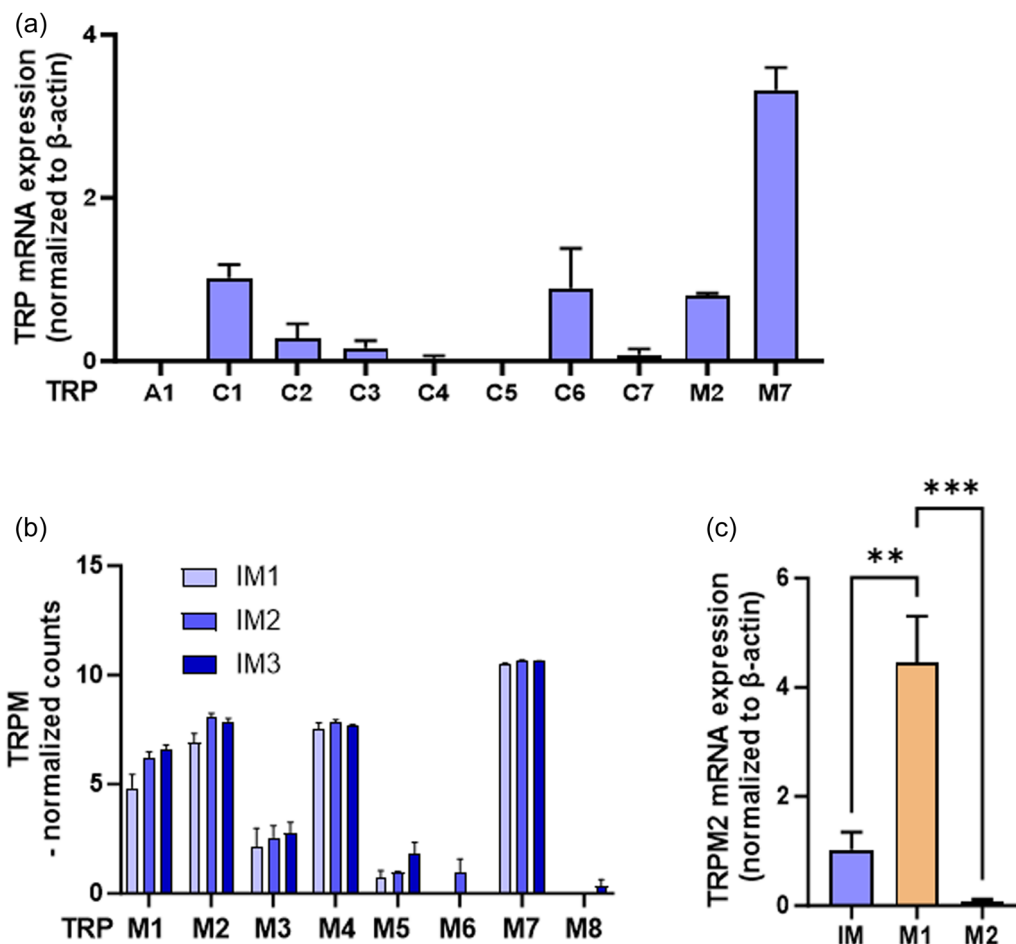


FIGURE 3 TRP expression in IMs. (a) mRNA levels of TRPA1, TRPC, TRPM2 and TRPM7 channels were quantified by quantitative RT-PCR. (b) Data for the mRNA expression of TRPM family genes as normalized counts from the three IM populations extracted from the bulk RNA-seq data set—GSE94135 (Gibbings et al., 2017). (c) Quantitative RT-PCR data for TRPM2 mRNA expression in unstimulated IMs (IM) and IMs polarized to the M1 (M1) or to the M2 state (M2). All samples are normalized to the expression of the housekeeping gene β -actin. $n = 3$ samples per group, $**p < 0.01$, $***p < 0.001$.

Information: Figure S1) denoting a high polarization rate in IMs detected with flow cytometry.

3.3 | TRP channels in IMs

TRP channels play a crucial role in functioning of immune cells in the body (Santoni et al., 2018; Froghi et al., 2021). TRPM2 is essential for monocytes (Yamamoto et al., 2008) as well as neutrophil function (Robledo-Avila et al., 2020), while TRPM7 is ubiquitously expressed in almost all cells of the body (Zou et al., 2019). TRPA1 is predominantly expressed in neuronal cells but was also detected in alveolar type II cells (Kannler et al., 2018). Therefore, we set out to identify TRP channel expression in IMs by quantifying mRNA levels of these TRP proteins (Figure 3a). As expected, no TRPA1 mRNA was detected, while TRPM7 mRNA was highly expressed. TRPC1 and TRPC6 as well as TRPM2 mRNA were identified in similar amounts (Figure 3a). We next analyzed TRPM mRNA expression levels in a publicly available bulk RNA-sequencing data set (NCBI data repository—GSE94135) of

the three identified IM species (Gibbings et al., 2017). TRPM2 mRNA showed a similar high expression pattern like TRPM1 and TRPM4 in all three IM species (Figure 3b). As TRPM2 controls polarization of gastric macrophages (Beceiro et al., 2017), we analyzed the mRNA expression of this channel in polarized IMs and identified a highly significant upregulation in the polarized M1 state compared to the unstimulated cells (Figure 3c). Moreover, polarization to the M2 state by IL-4 resulted in a significant downregulation of TRPM2 mRNA compared to unstimulated IM and polarized M1 cells. Therefore, polarization of IMs to the M1 state after application of LPS and IFN- γ induces TRPM2 mRNA expression.

3.4 | CD38 upregulation in TRPM2^{-/-} IM

Next, we quantified mRNAs of IM M1-specific surface marker proteins in TRPM2-deficient cells in comparison to WT cells. While SOCS3 (Figure 4a), CD86 (Figure 4b), and iNos (Figure 4c) were all upregulated in both cell types during M1 polarization in similar

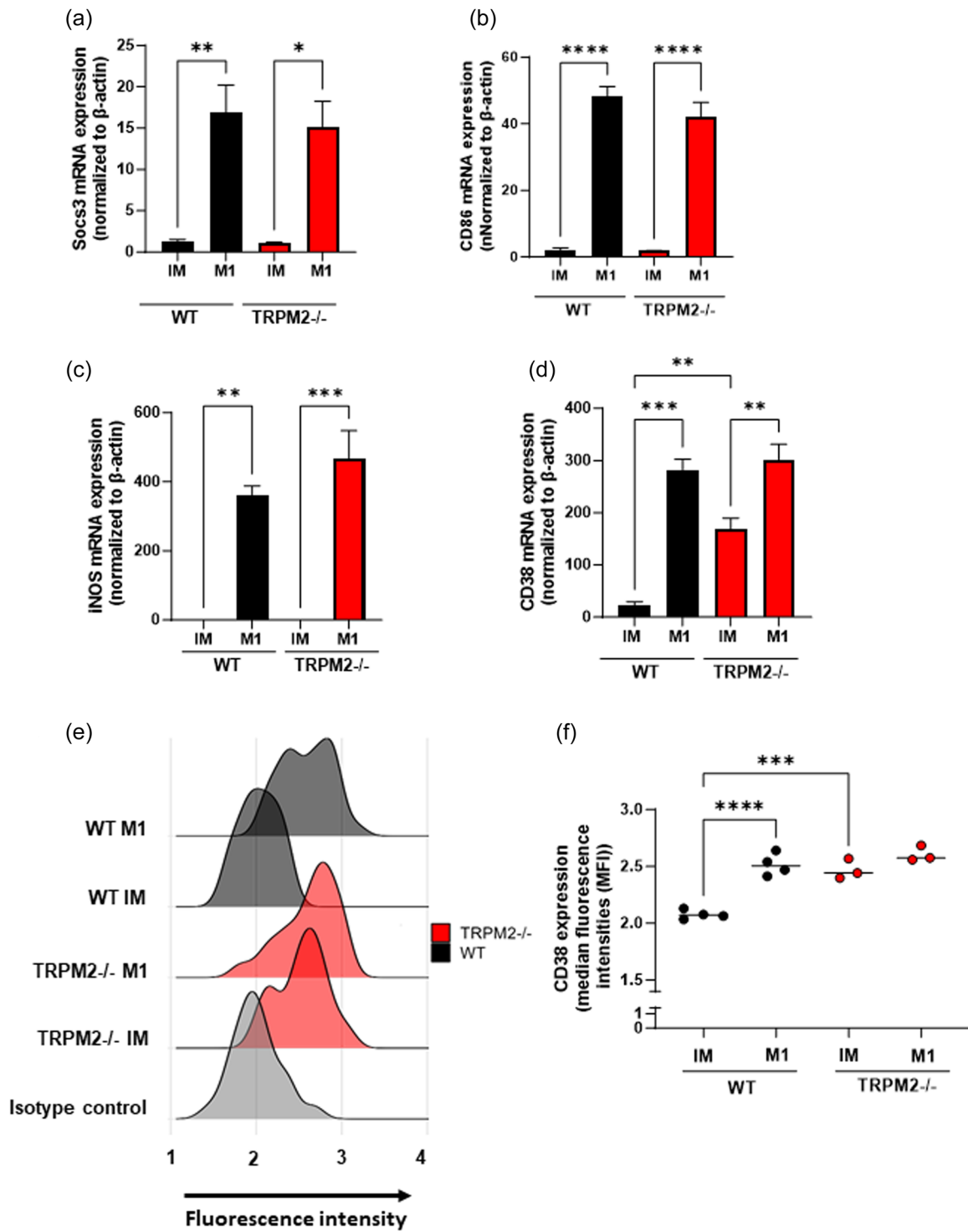


FIGURE 4 Characterization of M1 marker proteins in wild type (WT) and TRPM2-deficient (TRPM2^{-/-}) IMs. (a-d) Quantification of mRNA levels of marker proteins specific for the M1 state (Socs3 (a), CD86 (b), iNos (c), and CD38 (d)) in WT (black) and TRPM2^{-/-} (red) IMs. All samples are normalized to the expression of the housekeeping gene β -actin. (e) Representative histograms in a ridgeline plot obtained by flow cytometry after application of fluorescence-coupled anti CD38 antibodies to WT (in black) or TRPM2^{-/-} (in red) IMs (IM) and IMs polarized to the M1 state (M1). The application of isotype antibodies serves as negative control (in gray). (f) Quantification of CD38 expression by analyzing the median fluorescence intensities (MFI) in flow cytometry experiments shown in (e). $n = 3-4$ samples per group, * $p < 0.05$, ** $p < 0.01$, *** $p < 0.001$, **** $p < 0.0001$.

amounts, CD38 mRNA levels were already high in unstimulated TRPM2-deficient IMs and further increased during M1 polarization (Figure 4d). Most interestingly, CD38 is an ectoenzyme, which converts NAD⁺ or cyclic ADP-ribose into ADPR, a specific activator of TRPM2 channels (reviewed in Lund et al., 1998; Numata et al., 2012) and is predominantly expressed in IMs polarized to the M1 state (Supporting Information: Figure S1) with higher levels of TRPM2 mRNA (Figure 3c). In contrast to the qRT-PCR data, CD38 protein levels on the cell surface analyzed by flow cytometry with specific fluorescence-coupled CD38 antibodies in TRPM2-deficient IMs were not significantly different compared to TRPM2-deficient and WT IMs polarized to the M1 state (Figure 4e,f) for yet unknown reasons.

3.5 | Electrophysiology of TRPM2 channels in IM and M1 polarized IMs

To verify TRPM2 activity in these cells, we quantified ADPR-induced currents in unstimulated and M1-polarized WT as well as TRPM2-deficient IMs in voltage clamp experiments. ADPR added from the patch pipette, in general did not increase current densities (pA/pF) in WT IMs in between 80 s after whole-cell break-in ($n = 9$ of 10 cells), similar to TRPM2^{-/-} IMs polarized to the M1 state ($n = 6$ cells) (Figure 5a,c). After polarization of WT IMs to the M1 pro-inflammatory phenotype, ADPR-induced current densities significantly increased ($n = 10$ cells of 22) in contrast to WT IMs and TRPM2^{-/-} IMs polarized to the M1 state, confirming our previous result showing upregulation of TRPM2 in M1 polarized WT IMs (Figure 3c). These results were also evident in the IV (current-voltage) curve depicted in Figure 5b. A fraction (12 of 22 cells) of M1 polarized WT IMs, however, did not develop increased current densities after adding ADPR for unknown reasons.

3.6 | Inflammatory cytokine release in TRPM2^{-/-} IMs

An important function of IMs of the pro-inflammatory M1 state is the production of cytokines to attract other immune cells to the site invaded by pathogens (Aegerter et al., 2022). To test if TRPM2 is involved in the regulation of cytokine release by IMs, we polarized IMs isolated from WT and TRPM2^{-/-} mice to the M1 state after application of LPS and IFN- γ and quantified mRNA levels of inflammatory cytokines like TNF- α , IL-1 α and IL-6 using qRT-PCR. As expected, mRNA of levels of all three cytokines were upregulated in the M1 state of WT IMs, but most interestingly, a significantly higher expression was observed in TRPM2^{-/-} IMs (Figure 6a-c). To confirm these results on a protein level, we also quantified the release of cytokines in cell supernatants at 0, 1, 3, 6, and 24 h after polarization using specific ELISAs for all three cytokines. Again, all three cytokines were upregulated in the M1 state and were secreted in higher levels in TRPM2^{-/-} IMs (Figure 6d-f). While

TNF- α secretion was already significantly increased after 3 h in TRPM2^{-/-} IMs after application of LPS and IFN- γ , IL-6 followed after 6 h and IL-1 α after 24 h (Figure 6d-f). Therefore, deletion of TRPM2 in IMs, resulted in a higher upregulation of cytokine production and secretion compared to TRPM2-expressing WT cells.

3.7 | ROS production and membrane potentials in IMs

As cytokine production depends on ROS generation by nicotinamide adenine dinucleotide phosphate (NADPH)-oxidase (NOX) (Iles & Forman, 2002), which are closely regulated by the cell's membrane potentials. Our voltage clamp experiments (Figure 5) showed increases in current densities by TRPM2 channels only in M1-polarized WT IMs (Figure 5). Therefore, we analyzed changes in the membrane potential in current-clamp experiments in WT IMs of the M1 state. We were able to identify significantly higher membrane potentials by cation influx through TRPM2 channels after the application of ADPR in M1-polarized WT IMs (Figure 7a). Moreover, mRNA levels of NADPH oxidase 2 (NOX2) as the most predominantly expressed NOX isoform were significantly increased in IMs polarized to M1 from TRPM2^{-/-} mice compared to non-polarized IMs and IMs from WT mice (Figure 7b and Supporting information: Figure S2). Indeed, ROS production detected by a specific fluorescent dye (H₂DCFDA) was significantly higher in TRPM2^{-/-} IMs after 30 and 40 min of treatment with LPS and IFN- γ when compared to WT IMs (Figure 7c). As a consequence of higher ROS production, the ratio of reduced to oxidized glutathione (GSH/GSSG), a well-known marker for oxidative stress, is reduced (Yamada et al., 2006; Zitka et al., 2012). We observed a simultaneous ROS-dependent reduction of GSH/GSSG in both WT and TRPM2^{-/-} IMs. However, the decrease was significantly more pronounced in TRPM2^{-/-} IMs (Figure 7d). Addition of a NOX2 inhibitor, GSK2795039 (Hirano et al., 2015), diminishes the production of ROS in both WT and TRPM2^{-/-} IMs (Figure 7e). Hence, ablation of TRPM2 in IMs leads to higher ROS production, possibly orchestrated by NOX2, accompanied with a decline in GSH/GSSG ratios.

4 | DISCUSSION

Studying IMs was complicated, as viable isolated cell numbers were low, due to their remote location in lung tissues (Aegerter et al., 2022). Therefore, most of the studies characterized IM populations in the lung by fluorescence activated cell sorting followed by single-cell RNA-sequencing techniques (Chakarov et al., 2019; Gibbings et al., 2017; Schyns et al., 2018). However, for a more functional approach, increased numbers of viable cells are essential, which was achieved by coculturing IMs with stromal cells (Ogawa et al., 2019). We improved this published method by reducing the duration of coculture and by a magnetic separation with particles coupled to CD11b antibodies, which is less time-consuming (Figure 1a). It utilizes

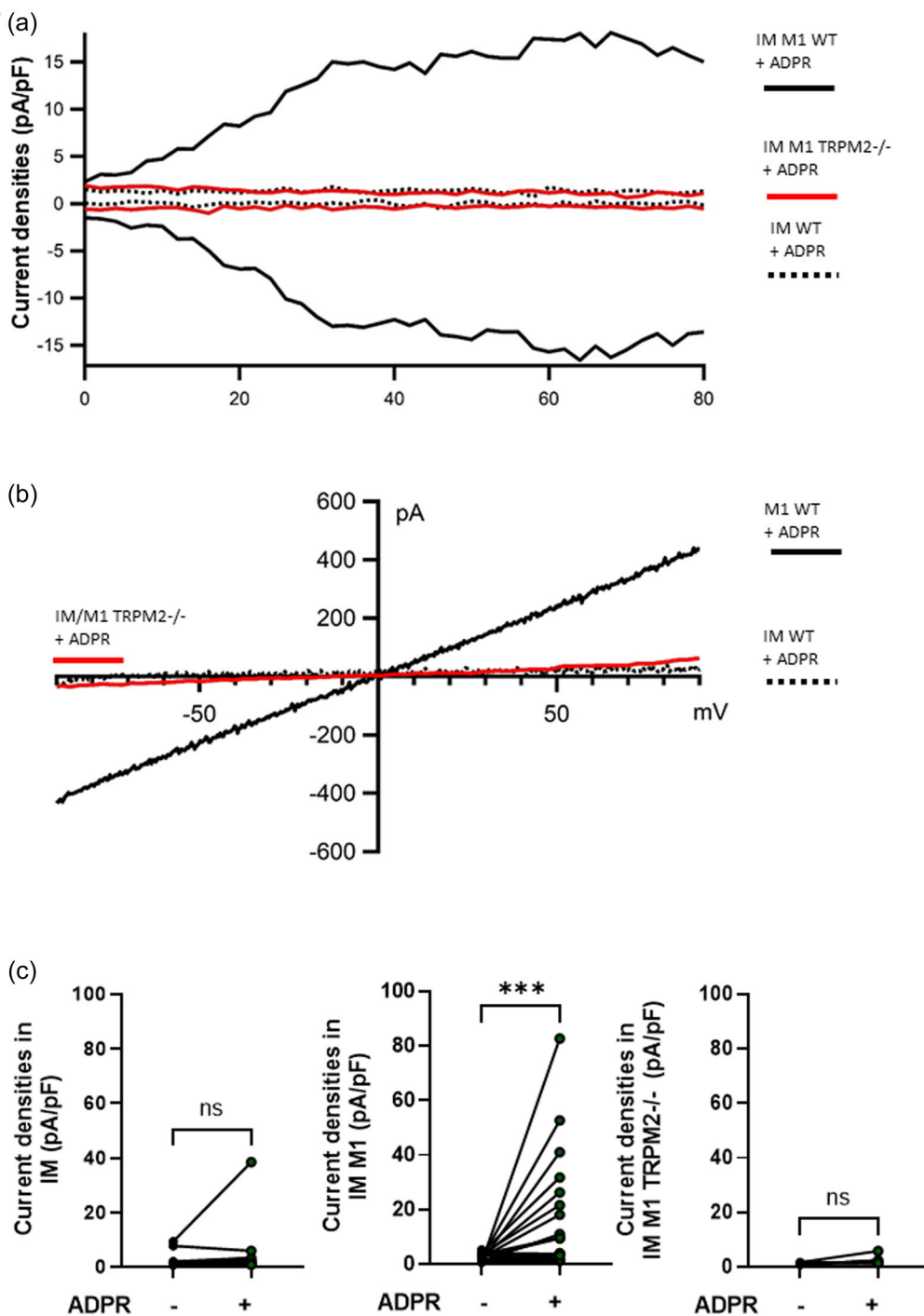


FIGURE 5 Electrophysiological characterization of TRPM2 currents in IMs induced by ADP-ribose (ADPR). (a) Current densities (pA/pF) in presence of ADPR in wild-type (WT) IMs (IM WT, black stippled line), M1 polarized IMs (IM M1 WT, black line), and TRPM2-deficient IMs polarized to the M1 state (IM M1 TRPM2^{-/-}, red line). Data from representative experiments are shown (for IM M1 WT, 10 of 22 cells). (b) IV (current–voltage) curve of maximum currents detected after application of ADPR in WT IMs (IM WT, black stippled line), M1 polarized IMs (IM M1 WT, black line), and TRPM2-deficient IMs polarized to the M1 state (IM M1 TRPM2^{-/-}, red line). Data from representative experiments are shown (for IM M1 WT, 10 of 22 cells). (c) Scatter plots summarizing changes in current densities of WT IMs (IM WT, *n* = 10) WT IMs polarized to the M1 state (IM M1 WT, *n* = 22) and TRPM2-deficient IMs polarized to the M1 state (IM M1 TRPM2^{-/-}, *n* = 6) before (black circles) and after (green circles) application of ADPR. Statistical analysis was performed by a Wilcoxon matched pairs signed rank test. *** *p* < 0.001.

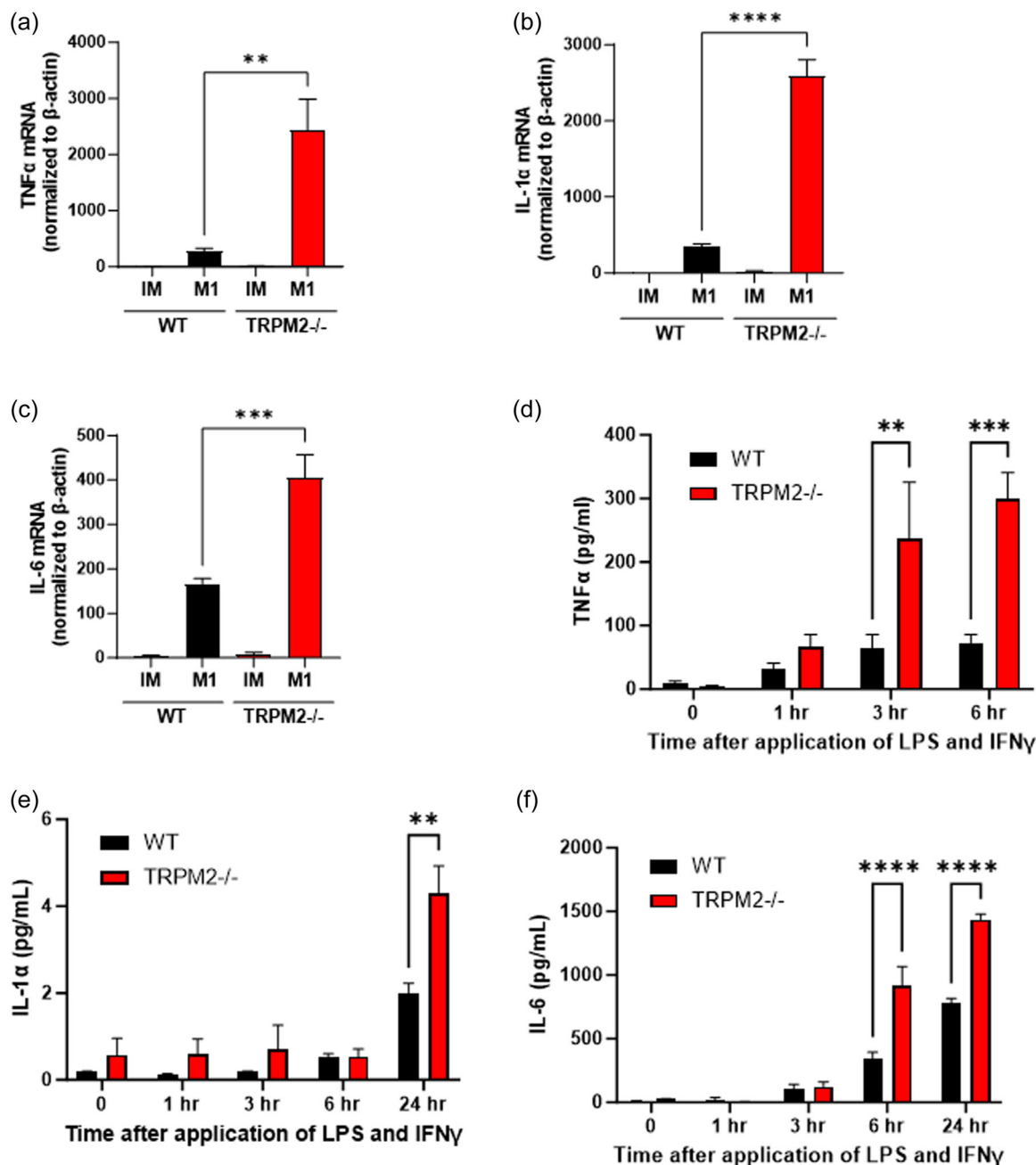


FIGURE 6 Cytokine production and secretion in unstimulated or M1 polarized wild-type (WT) and TRPM2-deficient (TRPM2^{-/-}) IMs. (a) mRNA levels of tumor necrosis factor α (TNF-α), (b) interleukin-1α (IL-1α), (c) Interleukin 6 (IL-6) were measured by quantitative RT-PCR and normalized to the expression of the housekeeping gene β-actin. (d) TNF-α, (e) IL-1α, and (f) IL-6 secretion after application of lipopolysaccharide (LPS) and interferon-γ (IFN-γ) was quantified by enzyme-linked immunosorbent assays (ELISAs) in the culture supernatant. $n = 3-4$ samples per group, ** $p < 0.01$, *** $p < 0.001$, **** $p < 0.0001$.

a murine IM-specific marker (reviewed in Gu et al., 2022), which is not present in closely related alveolar macrophages (AMs) removed by an initial bronchoalveolar lavage (Figure 1b,d). Moreover, mRNA for Csf1r as another IM-specific marker was expressed in our isolated IMs, while mRNA for the AM-specific Csf2rb was not detected (Figure 1e) and closely related dendritic cells do not express CD64 (Figure 1b) (Misharin et al., 2013). Thus, we hope that this isolation procedure, will stimulate research on IM function in the future. Like

AMs, IMs can be polarized to a pro-inflammatory M1 state and an anti-inflammatory M2 state for tissue repair (Tsurutani et al., 2021) in vitro to serve the needs of a closely regulated immune response. Successful polarization to both states was verified by an upregulation of mRNA expression of specific marker proteins (Figure 2b-f). Several reports showed evidence that these polarized states of IMs exist in vivo in challenged mice (Dumigan et al., 2022; Ji et al., 2014; Nie et al., 2017; Peng et al., 2024; Strickland et al., 2023), but the

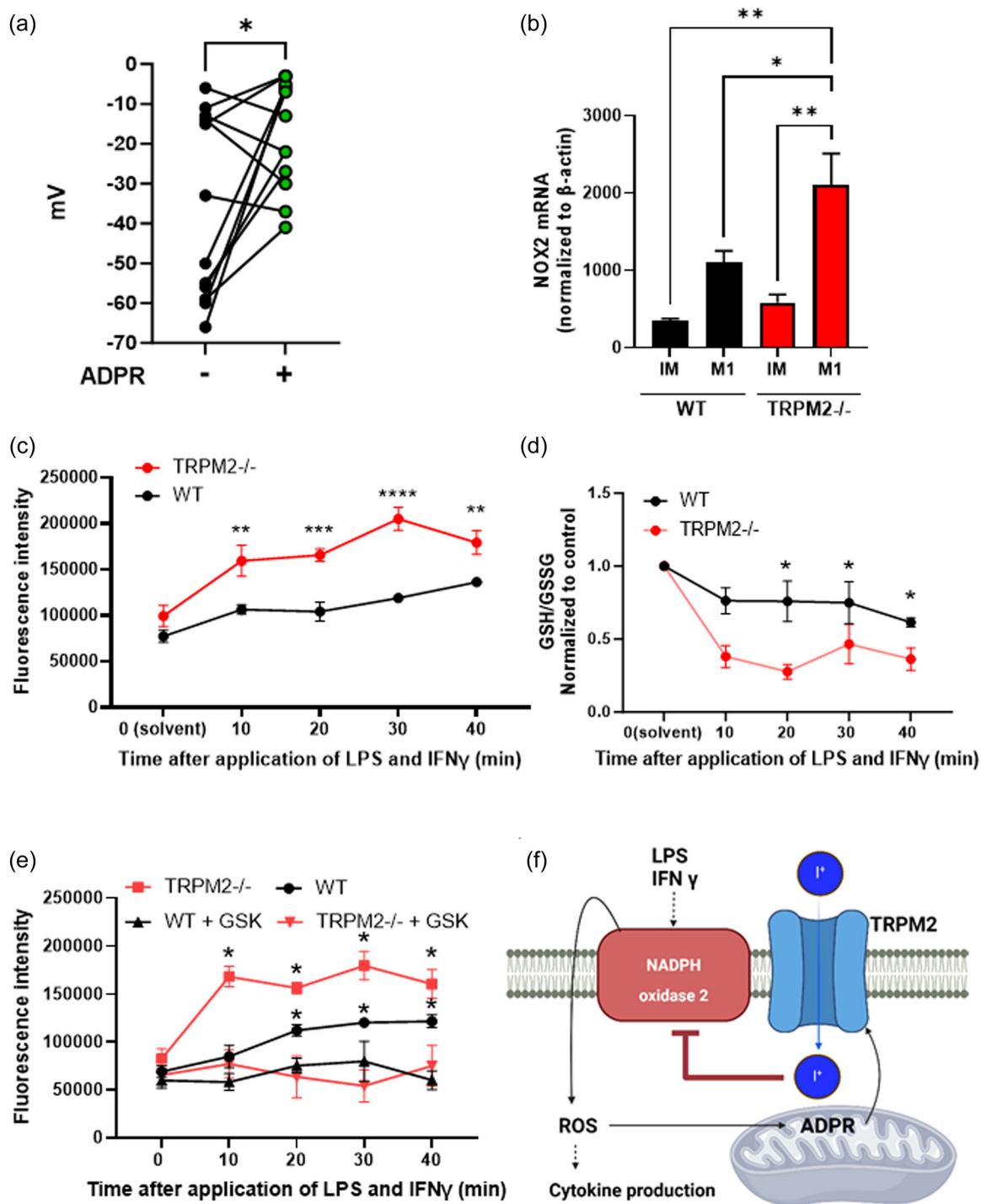


FIGURE 7 Membrane potentials and production of reactive oxygen species (ROS) in IMs. (a) Quantification of membrane potentials in IMs before (black circles) and after application of ADP-ribose (ADPR) (green circles). (b) Quantification of mRNA levels of the NADPH isoform 2 (NOX2) in IMs (IM) and IMs polarized to the M1 state (M1) from wild-type (WT, black columns) and TRPM2-deficient (TRPM2^{-/-}, red columns) mice. All samples are normalized to the expression of the housekeeping gene β -actin. (c) Detection of intracellular ROS levels by measuring fluorescence intensity of 2',7'-dichlorodihydrofluorescein diacetate (H₂DCFDA), (d) luminescence ratios of reduced to oxidized glutathione (GSH/GSSG), (e) with or without NOX2 inhibitor GSK2795039 following the application of lipopolysaccharide (LPS) and interferon- γ (IFN- γ) at various time points. (f) Schematic presentation of events inducing TRPM2-mediated inhibition of cytokine production and secretion. See text for more details. $n = 3-4$ samples per group, * $p < 0.05$ (in (e) to all other values), ** $p < 0.01$, *** $p < 0.001$, **** $p < 0.0001$.

exact mechanism of polarization of IMs in lung tissues remains elusive.

TRP channels are expressed in a variety of different cell types and serve multiple functions in the human body (Nilius & Szallasi, 2014). We detected mRNAs of two members of the TRPC family TRPC1 and TRPC6 together with TRPM2 and TRPM7 in the isolated IMs. Using bulk RNA-sequencing data from a publication characterizing three different populations of IMs (Gibbings et al., 2017), we were able to analyze the transcriptome profile of IMs, including members of the TRPM gene family (Chubanov et al., 2024). TRPM2 next to TRPM4 mRNA was highly expressed in all three IM populations (Figure 3b). As TRPM2 serves an important role in monocytes and other immune cells (reviewed in Faouzi & Penner, 2014), we started to study this channel utilizing a TRPM2-deficient mouse model (Yamamoto et al., 2008). TRPM2^{-/-} IM cells were successfully polarized to the M1 state as demonstrated by an upregulation of mRNAs for M1-specific marker proteins (Figure 4a-c). However, CD38 as an additional marker protein was already upregulated in unstimulated IMs (Figure 4d-f). CD38 is an ectoenzyme converting NAD⁺ in ADPR (reviewed in Chini et al., 2020; Guerreiro et al., 2020), a specific activator of TRPM2 channels (Numata et al., 2012; reviewed in Faouzi & Penner, 2014). ADPR production by CD38, next to generation in mitochondria as well as poly(ADPR) polymerase (PARP) and poly(ADPR) glycohydrolase (PARG) in the nucleus, is indeed able to activate TRPM2 channels in living cells (reviewed in Faouzi & Penner, 2014). Although TRPM2-deficient IMs express higher levels of CD38, changes in other markers like iNos, Socs3, and CD86 remain comparable to WT (Figure 4a-d). Moreover, the basal level of cytokine secretion is still lower than in the stimulated states (Figure 6d-f). Together, these findings denote that TRPM2^{-/-} IMs remain unpolarized in steady-state. Mechanistically, TRPM2 channels might downregulate CD38 in unstimulated IMs by a yet unknown mechanism to avoid over-production of ADPR and over-activation of the channels by a negative feedback loop, which needs to be dissected further. Importantly, TRPM2 mRNA was not only expressed in unstimulated IMs, but significantly upregulated after polarization to the M1, but not to the M2 state (Figure 3c).

As identification of endogenous TRPM2 channels with antibodies remains challenging and can be misleading, we relayed on a functional approach by quantifying TRPM2 currents induced by the well-studied activator ADPR (Perraud et al., 2001). Application of ADPR induced strong currents in IMs polarized to the M1 state, which was significantly lower in unstimulated IMs and absent in TRPM2^{-/-} cells (Figure 5a,b). To the best of our knowledge, we present here the first successful patch-clamp recordings of specific TRPM2 currents in IMs in the whole-cell mode confirming an upregulation of TRPM2 proteins in the M1 state.

The innate immune response of macrophages against invading micro-organisms is the immediate release of pro-inflammatory cytokines. When infected with *H. pylori*, the resident macrophages isolated from the gastric mucosa of TRPM2^{-/-} mice showed

augmented levels of pro-inflammatory cytokines (Beceiro et al., 2017). Moreover, on a functional basis, IMs are rather important for cytokine production than for phagocytosis, which is the main task of AMs in the alveolus (Aegerter et al., 2022). Therefore, we quantified cytokine mRNA expression and secretion in unstimulated and M1-polarized IMs. Surprisingly, cytokine production and secretion to the extracellular medium were significantly higher in TRPM2-deficient IMs polarized to the M1 state in comparison to WT cells (Figure 6a-f). When the phagocytes are subjected to oxidative stress, there is an increase in ROS generation which consequently activates the transcription of nuclear factor-kappa-light-chain-enhancer of activated B-cells (NF-κB) as one of its downstream effects. This activation initiates a positive feedback loop of continuous ROS generation by NADPH oxidase (Anrather et al., 2006; Morgan & Liu, 2011) ultimately leading to increased expression of pro-inflammatory cytokines (Lawrence, 2009). Cytokine production is strictly correlated to ROS production via coupling an unbalanced glutathione redox status to activation of NF-κB signaling (reviewed in Filippin et al., 2008). In the initial stages of host defense against infection, circulating neutrophils migrate to the site and eventually, induce respiratory burst to release ROS for bactericidal functions. TRPM2 has already been linked with this process of respiratory burst in neutrophils (Yamamoto et al., 2008). Concomitantly, low-grade respiratory bursts have also been reported in macrophages and rather for intracellular signaling than for killing of bacteria (Iles & Forman, 2002). As TRPM2 is a key player in ROS-mediated signaling in various cell types and pathologies like cancer and ischemic stroke (reviewed in Maliougina & El Hiani, 2023), the next step was to measure the levels of ROS in IMs. LPS and IFN-γ-induced ROS production in M1 polarized IMs was higher (Figure 7c) and GSH/GSSG levels were suppressed in TRPM2^{-/-} cells (Figure 7d). Our study demonstrates that TRPM2 plays an essential role in the regulation of ROS production in IMs and confirms previous data in cardiomyocytes, where Ca²⁺ influx via TRPM2 is essentially required for the reduction of oxidative stress (Hoffman et al., 2015).

As ROS production by NADPH oxidases is inhibited by increases in the cell membrane potential (DeCoursey, 2003; Petheo & Demarex, 2005), we quantified membrane potentials in IMs before and after application of ADPR. Indeed, membrane potentials were significantly higher in cells after TRPM2 activation by ADPR (Figure 7a), most probably by an enhanced cation influx through the channels. Most interestingly, a similar observation was reported in bone marrow-derived macrophages (BMDMs) after stimulation with LPS (Di et al., 2011). ADPR can be released from mitochondria by ROS, especially by ROS-produced H₂O₂ and activate TRPM2 channels (Ayub & Hallett, 2004; Perraud et al., 2005) to inhibit NADPH oxidase by membrane depolarization. Importantly, mRNA levels of NADPH oxidase 2 (NOX2) as the most predominantly expressed NOX isoform were significantly increased in TRPM2^{-/-} IMs polarized to M1 (Figure 7b), pointing to an inhibitory role of TRPM2 channels also on the transcriptional level. Reduction of NOX expression and activity will reduce the generation of ROS and

cytokine production as well as its secretion (see Figure 7f). Our data are therefore another example of a rather beneficial than detrimental effect of TRPM2 channels following oxidative stress (as reviewed in Maliougina & El Hiani, 2023; Miller & Cheung, 2016).

5 | CONCLUSIONS

In summary, we introduced an efficient method to isolate IMs from mouse models, polarized them to the pro-inflammatory M1 state and were able to identify ADPR-induced TRPM2 currents, but not in TRPM2-deficient IMs. Surprisingly, cytokine production and secretion were exacerbated in TRPM2^{-/-} IMs, pointing to an important regulatory function of the redox-sensitive TRPM2 channels for cytokine release from IMs. Overproduction and secretion of cytokines by immune cells were recently described as a “cytokine storm” in COVID-19 patients, resulting in increased mortality. Therefore, previous data in BMDMs (Di et al., 2011) and our findings in IMs might be the basis for an efficient therapeutic option with TRPM2 channel activators to mitigate cytokine-induced pathologies in these patients in the future.

AUTHOR CONTRIBUTIONS

Alexander Dietrich contributed to the conception, design and funding of the study, interpreted the data, wrote the manuscript, and finally approved the submission. Suhasini Rajan was responsible for most of the experiments, data collection, coordinated its progress and research direction and wrote the manuscript draft. Vladimir Chubanov and Alexey Shalygin were responsible for patch-clamp experiments. Thomas Gudermann reviewed and revised the final manuscript. All authors have read and agreed to submit the final manuscript.

ACKNOWLEDGMENTS

We thank Dr. Yasuo Mori (Kyoto University, Japan) for sharing his TRPM2-deficient mouse model with us. We would like to acknowledge Ananya Kadekar for her assistance in the lab and Raffaele Conca for helping with sorting IMs. A. D., S. R., V. C., and T. G. were supported by the Deutsche Forschungsgemeinschaft (DFG) (TRR 152 [P15, P16] and GRK 2338 RTG [P04, P10]) and the German Center for Lung Research (DZL). Open Access funding enabled and organized by Projekt DEAL.

CONFLICT OF INTEREST STATEMENT

The authors declare no conflict of interest.

ETHICS STATEMENT

Tissue extraction from mouse models was approved by the regional authorities (Regierung Oberbayern).

ORCID

Suhasini Rajan  <http://orcid.org/0009-0009-6088-0293>

Alexander Dietrich  <http://orcid.org/0000-0002-1168-8707>

REFERENCES

- Aegerter, H., Lambrecht, B. N., & Jakubzick, C. V. (2022). Biology of lung macrophages in health and disease. *Immunity*, 55(9), 1564–1580. <https://doi.org/10.1016/j.immuni.2022.08.010>
- Anrather, J., Racchumi, G., & Iadecola, C. (2006). NF-κB regulates phagocytic NADPH oxidase by inducing the expression of gp91. *Journal of Biological Chemistry*, 281(9), 5657–5667. <https://doi.org/10.1074/jbc.M506172200>
- Ayub, K., & Hallett, M. B. (2004). The mitochondrial ADPR link between Ca²⁺ store release and Ca²⁺ influx channel opening in immune cells. *The FASEB Journal*, 18(12), 1335–1338. <https://doi.org/10.1096/fj.04-1888hyp>
- Beceiro, S., Radin, J. N., Chaturvedi, R., Piazuolo, M. B., Horvarth, D. J., Cortado, H., Gu, Y., Dixon, B., Gu, C., Lange, I., Koomoa, D. L., Wilson, K. T., Algood, H. M. S., & Partida-Sánchez, S. (2017). TRPM2 ion channels regulate macrophage polarization and gastric inflammation during *Helicobacter pylori* infection. *Mucosal Immunology*, 10(2), 493–507. <https://doi.org/10.1038/mi.2016.60>
- Bedoret, D., Wallemacq, H., Marichal, T., Desmet, C., Quesada Calvo, F., Henry, E., Closset, R., Dewals, B., Thielen, C., Gustin, P., de Leval, L., Van Rooijen, N., Le Moine, A., Vanderplasschen, A., Cataldo, D., Drion, P. V., Moser, M., Lekeux, P., & Bureau, F. (2009). Lung interstitial macrophages alter dendritic cell functions to prevent airway allergy in mice. *Journal of Clinical Investigation*, 119(12), 3723–3738. <https://doi.org/10.1172/JCI39717>
- Chakarov, S., Lim, H. Y., Tan, L., Lim, S. Y., See, P., Lum, J., Zhang, X. M., Foo, S., Nakamizo, S., Duan, K., Kong, W. T., Gentek, R., Balachander, A., Carbajo, D., Blieriot, C., Malleret, B., Tam, J. K. C., Baig, S., Shabeer, M., ... Ginhoux, F. (2019). Two distinct interstitial macrophage populations coexist across tissues in specific subtissular niches. *Science*, 363(6432), eaau0964. <https://doi.org/10.1126/science.aau0964>
- Cheng, P., Li, S., & Chen, H. (2021). Macrophages in lung injury, repair, and fibrosis. *Cells*, 10(2), 436. <https://doi.org/10.3390/cells10020436>
- Chini, C. C. S., Peclat, T. R., Warner, G. M., Kashyap, S., Espindola-Netto, J. M., de Oliveira, G. C., Gomez, L. S., Hogan, K. A., Tarragó, M. G., Puranik, A. S., Agorrody, G., Thompson, K. L., Dang, K., Clarke, S., Childs, B. G., Kanamori, K. S., Witte, M. A., Vidal, P., Kirkland, A. L., ... Chini, E. N. (2020). CD38 ecto-enzyme in immune cells is induced during aging and regulates NAD(+) and NMN levels. *Nature Metabolism*, 2(11), 1284–1304. <https://doi.org/10.1038/s42255-020-00298-z>
- Chubanov, V., Köttgen, M., Touyz, R. M., & Gudermann, T. (2024). TRPM channels in health and disease. *Nature Reviews Nephrology*, 20(3), 175–187. <https://doi.org/10.1038/s41581-023-00777-y>
- DeCoursey, T. E. (2003). Interactions between NADPH oxidase and voltage-gated proton channels: Why electron transport depends on proton transport. *FEBS Letters*, 555(1), 57–61. [https://doi.org/10.1016/s0014-5793\(03\)01103-7](https://doi.org/10.1016/s0014-5793(03)01103-7)
- Di, A., Gao, X. P., Qian, F., Kawamura, T., Han, J., Hecquet, C., Ye, R. D., Vogel, S. M., & Malik, A. B. (2011). The redox-sensitive cation channel TRPM2 modulates phagocyte ROS production and inflammation. *Nature Immunology*, 13(1), 29–34. <https://doi.org/10.1038/ni.2171>
- Dumigan, A., Cappa, O., Morris, B., Sá Pessoa, J., Calderon-Gonzalez, R., Mills, G., Lancaster, R., Simpson, D., Kissenpennig, A., & Bengoechea, J. A. (2022). In vivo single-cell transcriptomics reveal *Klebsiella pneumoniae* skews lung macrophages to promote infection. *EMBO Molecular Medicine*, 14(12), e16888. <https://doi.org/10.15252/emmm.202216888>
- Faouzi, M., & Penner, R. (2014). Trpm2. *Handbook of Experimental Pharmacology*, 222, 403–426. https://doi.org/10.1007/978-3-642-54215-2_16
- Filippin, L. I., Vercellino, R., Marroni, N. P., & Xavier, R. M. (2008). Redox signalling and the inflammatory response in rheumatoid arthritis.

- Clinical and Experimental Immunology*, 152(3), 415–422. <https://doi.org/10.1111/j.1365-2249.2008.03634.x>
- Fliegert, R., Watt, J. M., Schöbel, A., Rozewicz, M. D., Moreau, C., Kirchberger, T., Thomas, M. P., Sick, W., Araujo, A. C., Harneit, A., Potter, B. V. L., & Guse, A. H. (2017). Ligand-induced activation of human TRPM2 requires the terminal ribose of ADPR and involves Arg1433 and Tyr1349. *Biochemical Journal*, 474(13), 2159–2175. <https://doi.org/10.1042/BCJ20170091>
- Froghi, S., Grant, C. R., Tandon, R., Quaglia, A., Davidson, B., & Fuller, B. (2021). New insights on the role of TRP channels in calcium signalling and immunomodulation: Review of pathways and implications for clinical practice. *Clinical Reviews in Allergy & Immunology*, 60(2), 271–292. <https://doi.org/10.1007/s12016-020-08824-3>
- Gibbins, S. L., Thomas, S. M., Atif, S. M., McCubbrey, A. L., Desch, A. N., Danhorn, T., Leach, S. M., Bratton, D. L., Henson, P. M., Janssen, W. J., & Jakubczik, C. V. (2017). Three unique interstitial macrophages in the murine lung at steady state. *American Journal of Respiratory Cell and Molecular Biology*, 57(1), 66–76. <https://doi.org/10.1165/rcmb.2016-0361OC>
- Gu, Y., Lawrence, T., Mohamed, R., Liang, Y., & Yahaya, B. H. (2022). The emerging roles of interstitial macrophages in pulmonary fibrosis: A perspective from scRNA-seq analyses. *Frontiers in Immunology*, 13:923235. <https://doi.org/10.3389/fimmu.2022.923235>
- Guerreiro, S., Privat, A. L., Bressac, L., & Toulorge, D. (2020). CD38 in neurodegeneration and neuroinflammation. *Cells*, 9(2), 471. <https://doi.org/10.3390/cells9020471>
- Guilliams, M., De Kleer, I., Henri, R., Post, S., Vanhoutte, L., De Prijck, S., Deswarte, K., Malissen, B., Hammad, H., & Lambrecht, B. N. (2013). Alveolar macrophages develop from fetal monocytes that differentiate into long-lived cells in the first week of life via GM-CSF. *Journal of Experimental Medicine*, 210(10), 1977–1992. <https://doi.org/10.1084/jem.20131199>
- Hirano, K., Chen, W. S., Chueng, A. L., Dunne, A. A., Seredenina, T., Filippova, A., Ramachandran, S., Bridges, A., Chaudry, L., Pettman, G., Allan, C., Duncan, S., Lee, K. C., Lim, J., Ma, M. T., Ong, A. B., Ye, N. Y., Nasir, S., Mulyanidewi, S., ... Rutter, A. R. (2015). Discovery of GSK2795039, a novel small molecule NADPH oxidase 2 inhibitor. *Antioxidants & Redox Signaling*, 23(5), 358–374. <https://doi.org/10.1089/ars.2014.6202>
- Hoeffel, G., Chen, J., Lavin, Y., Low, D., Almeida, F. F., See, P., Beaudin, A. E., Lum, J., Low, I., Forsberg, E. C., Poidinger, M., Zolezzi, F., Larbi, A., Ng, L. G., Chan, J. K. Y., Greter, M., Becher, B., Samokhvalov, I. M., Merad, M., & Ginhoux, F. (2015). C-Myb(+) erythro-myeloid progenitor-derived fetal monocytes give rise to adult tissue-resident macrophages. *Immunity*, 42(4), 665–678. <https://doi.org/10.1016/j.immuni.2015.03.011>
- Hoffman, N. E., Miller, B. A., Wang, J., Elrod, J. W., Rajan, S., Gao, E., & Cheung, J. Y. (2015). Ca²⁺(+) entry via Trpm2 is essential for cardiac myocyte bioenergetics maintenance. *American Journal of Physiology: Heart and Circulatory Physiology*, 308(6), H637–H650. <https://doi.org/10.1152/ajpheart.00720.2014>
- Iles, K. E., & Forman, H. J. (2002). Macrophage signaling and respiratory burst. *Immunologic Research*, 26(1–3), 095–106. <https://doi.org/10.1385/IR.26:1-3:095>
- Jablonski, K. A., Amici, S. A., Webb, L. M., Ruiz-Rosado, J. D., Popovich, P. G., Partida-Sanchez, S., & Guerau-de-Arellano, M. (2015). Novel markers to delineate murine M1 and M2 macrophages. *PLoS One*, 10(12), e0145342. <https://doi.org/10.1371/journal.pone.0145342>
- Ji, W. J., Ma, Y. Q., Zhou, X., Zhang, Y. D., Lu, R. Y., Sun, H. Y., Guo, Z. Z., Zhang, Z., Li, Y. M., & Wei, L. Q. (2014). Temporal and spatial characterization of mononuclear phagocytes in circulating, lung alveolar and interstitial compartments in a mouse model of bleomycin-induced pulmonary injury. *Journal of Immunological Methods*, 403(1–2), 7–16. <https://doi.org/10.1016/j.jim.2013.11.012>
- Kamm, G. B., Boffi, J. C., Zuza, K., Nencini, S., Campos, J., Schrenk-Siemens, K., Sonntag, I., Kabaoğlu, B., El Hay, M. Y. A., Schwarz, Y., Tappe-Theodor, A., Bruns, D., Acuna, C., Kuner, T., & Siemens, J. (2021). A synaptic temperature sensor for body cooling. *Neuron*, 109(20), 3283–3297, e3211. <https://doi.org/10.1016/j.neuron.2021.10.001>
- Kannler, M., Luling, R., Yildirim, A. O., Gudermann, T., Steinritz, D., & Dietrich, A. (2018). TRPA1 channels: Expression in non-neuronal murine lung tissues and dispensability for hyperoxia-induced alveolar epithelial hyperplasia. *Pflügers Archiv: European Journal of Physiology*, 470, 1231–1241. <https://doi.org/10.1007/s00424-018-2148-6>
- Lawrence, T. (2009). The nuclear factor NF- κ B pathway in inflammation. *Cold Spring Harbor Perspectives in Biology*, 1(6), a001651. <https://doi.org/10.1101/cshperspect.a001651>
- Lei, F., Cui, N., Zhou, C., Chodosh, J., Vavvas, D. G., & Paschalis, E. I. (2020). CSF1R inhibition by a small-molecule inhibitor is not microglia specific; affecting hematopoiesis and the function of macrophages. *Proceedings of the National Academy of Sciences*, 117(38), 23336–23338. <https://doi.org/10.1073/pnas.1922788117>
- Li, W., Liang, L., Liao, Q., Li, Y., & Zhou, Y. (2022). CD38: An important regulator of T cell function. *Biomedicine & Pharmacotherapy*, 153:113395. <https://doi.org/10.1016/j.biopha.2022.113395>
- Lund, F. E., Cockayne, D. A., Randall, T. D., Solvason, N., Schuber, F., & Howard, M. C. (1998). CD38: A new paradigm in lymphocyte activation and signal transduction. *Immunological Reviews*, 161, 79–93. <https://doi.org/10.1111/j.1600-065x.1998.tb01573.x>
- Maliougina, M., & El Hiani, Y. (2023). TRPM2: Bridging calcium and ROS signaling pathways-implications for human diseases. *Frontiers in Physiology*, 14, 1217828. <https://doi.org/10.3389/fphys.2023.1217828>
- Mederos, Y. S. M., Waring, J., Gudermann, T., & Chubanov, V. (2008). Evolutionary determinants of divergent calcium selectivity of TRPM channels. *FASEB Journal*, 22, 1540. <https://doi.org/10.1096/fj.07-9694com>
- Meziani, L., Mondini, M., Petit, B., Boissonnas, A., Thomas de Montpreville, V., Mercier, O., Vozenin, M. C., & Deutsch, E. (2018). CSF1R inhibition prevents radiation pulmonary fibrosis by depletion of interstitial macrophages. *European Respiratory Journal*, 51(3), 1702120. <https://doi.org/10.1183/13993003.02120-2017>
- Miller, B. A., & Cheung, J. Y. (2016). TRPM2 protects against tissue damage following oxidative stress and ischaemia-reperfusion. *The Journal of Physiology*, 594(15), 4181–4191. <https://doi.org/10.1113/JP270934>
- Misharin, A. V., Morales-Nebreda, L., Mutlu, G. M., Budinger, G. R. S., & Perlman, H. (2013). Flow cytometric analysis of macrophages and dendritic cell subsets in the mouse lung. *American Journal of Respiratory Cell and Molecular Biology*, 49(4), 503–510. <https://doi.org/10.1165/rcmb.2013-0086MA>
- Morgan, M. J., & Liu, Z. (2011). Crosstalk of reactive oxygen species and NF- κ B signaling. *Cell Research*, 21(1), 103–115. <https://doi.org/10.1038/cr.2010.178>
- Nie, H., Wang, A., He, Q., Yang, Q., Liu, L., Zhang, G., Huang, Y., Ding, X., Yu, H., & Hu, S. (2017). Phenotypic switch in lung interstitial macrophage polarization in an ovalbumin-induced mouse model of asthma. *Experimental and Therapeutic Medicine*, 14(2), 1284–1292. <https://doi.org/10.3892/etm.2017.4699>
- Nilius, B., & Szallasi, A. (2014). Transient receptor potential channels as drug targets: From the science of basic research to the art of Medicine. *Pharmacological Reviews*, 66(3), 676–814. <https://doi.org/10.1124/pr.113.008268>

- Numata, T., Sato, K., Christmann, J., Marx, R., Mori, Y., Okada, Y., & Wehner, F. (2012). The ΔC splice-variant of TRPM2 is the hypertonicity-induced cation channel in HeLa cells, and the ectoenzyme CD38 mediates its activation. *The Journal of Physiology*, 590(5), 1121–1138. <https://doi.org/10.1113/jphysiol.2011.220947>
- Ogawa, K., Tsurutani, M., Hashimoto, A., & Soeda, M. (2019). Simple propagation method for resident macrophages by co-culture and subculture, and their isolation from various organs. *BMC Immunology*, 20(1), 34. <https://doi.org/10.1186/s12865-019-0314-z>
- Peng, Y., Qiao, S., Wang, H., Shekhar, S., Wang, S., Yang, J., Fan, Y., & Yang, X. (2024). Enhancement of macrophage immunity against chlamydial infection by natural killer T cells. *Cells*, 13(2), 133. <https://doi.org/10.3390/cells13020133>
- Perraud, A. L., Fleig, A., Dunn, C. A., Bagley, L. A., Launay, P., Schmitz, C., Stokes, A. J., Zhu, Q., Bessman, M. J., Penner, R., Kinet, J. P., & Scharenberg, A. M. (2001). ADP-ribose gating of the calcium-permeable LTRPC2 channel revealed by nudix motif homology. *Nature*, 411(6837), 595–599.
- Perraud, A. L., Takanishi, C. L., Shen, B., Kang, S., Smith, M. K., Schmitz, C., Knowles, H. M., Ferraris, D., Li, W., Zhang, J., Stoddard, B. L., & Scharenberg, A. M. (2005). Accumulation of free ADP-ribose from mitochondria mediates oxidative stress-induced gating of TRPM2 cation channels. *Journal of Biological Chemistry*, 280(7), 6138–6148.
- Petheo, G. L., & Demaurex, N. (2005). Voltage- and NADPH-dependence of electron currents generated by the phagocytic NADPH oxidase. *Biochemistry Journal*, 388(Pt 2), 485–491. <https://doi.org/10.1042/BJ20041889>
- Robledo-Avila, F. H., Ruiz-Rosado, J. D., Brockman, K. L., & Partida-Sánchez, S. (2020). The TRPM2 ion channel regulates inflammatory functions of neutrophils during listeria monocytogenes infection. *Frontiers in Immunology*, 11, 97. <https://doi.org/10.3389/fimmu.2020.00097>
- Santoni, G., Morelli, M. B., Amantini, C., Santoni, M., Nabissi, M., Marinelli, O., & Santoni, A. (2018). “Immuno-Transient receptor potential ion channels”: The role in monocyte- and macrophage-mediated inflammatory responses. *Frontiers in Immunology*, 9, 1273. <https://doi.org/10.3389/fimmu.2018.01273>
- Schyns, J., Bureau, F., & Marichal, T. (2018). Lung interstitial macrophages: Past, present, and future. *Journal of Immunology Research*, 2018, 5160794. <https://doi.org/10.1155/2018/5160794>
- Sheng, J., Ruedl, C., & Karjalainen, K. (2015). Most Tissue-Resident macrophages except microglia are derived from fetal hematopoietic stem cells. *Immunity*, 43(2), 382–393. <https://doi.org/10.1016/j.immuni.2015.07.016>
- Song, K., Wang, H., Kamm, G. B., Pohle, J., Reis, F. C., Heppenstall, P., Wende, H., & Siemens, J. (2016). The TRPM2 channel is a hypothalamic heat sensor that limits fever and can drive hypothermia. *Science*, 353(6306), 1393–1398. <https://doi.org/10.1126/science.aaf7537>
- Strickland, A. B., Chen, Y., Sun, D., & Shi, M. (2023). Alternatively activated lung alveolar and interstitial macrophages promote fungal growth. *iScience*, 26(5), 106717. <https://doi.org/10.1016/j.isci.2023.106717>
- Syed Mortadza, S. A., Wang, L., Li, D., & Jiang, L. H. (2015). TRPM2 channel-mediated ROS-sensitive Ca(2+) signaling mechanisms in immune cells. *Frontiers in Immunology*, 6, 407. <https://doi.org/10.3389/fimmu.2015.00407>
- Tsurutani, M., Horie, H., & Ogawa, K. (2021). Cell properties of lung tissue-resident macrophages propagated by co-culture with lung fibroblastic cells from C57BL/6 and BALB/c mice. *Biomedicine*, 9(9), 1241. <https://doi.org/10.3390/biomedicine9091241>
- Yamada, H., Arai, T., Endo, N., Yamashita, K., Fukuda, K., Sasada, M., & Uchiyama, T. (2006). LPS-induced ROS generation and changes in glutathione level and their relation to the maturation of human monocyte-derived dendritic cells. *Life Sciences*, 78(9), 926–933. <https://doi.org/10.1016/j.lfs.2005.05.106>
- Yamamoto, S., Shimizu, S., Kiyonaka, S., Takahashi, N., Wajima, T., Hara, Y., Negoro, T., Hiroi, T., Kiuchi, Y., Okada, T., Kaneko, S., Lange, I., Fleig, A., Penner, R., Nishi, M., Takeshima, H., & Mori, Y. (2008). TRPM2-mediated Ca²⁺-influx induces chemokine production in monocytes that aggravates inflammatory neutrophil infiltration. *Nature Medicine*, 14(7), 738–747. <https://doi.org/10.1038/nm1758>
- Zitka, O., Skalickova, S., Gumulec, J., Masarik, M., Adam, V., Hubalek, J., Trnkova, L., Kruseova, J., Eckschlager, T., & Kizek, R. (2012). Redox status expressed as GSH:GSSG ratio as a marker for oxidative stress in paediatric tumour patients. *Oncology Letters*, 4(6), 1247–1253. <https://doi.org/10.3892/ol.2012.931>
- Zou, Z. G., Rios, F. J., Montezano, A. C., & Touyz, R. M. (2019). TRPM7, magnesium, and signaling. *International Journal of Molecular Sciences*, 20(8), 1877. <https://doi.org/10.3390/ijms20081877>

SUPPORTING INFORMATION

Additional supporting information can be found online in the Supporting Information section at the end of this article.

How to cite this article: Rajan, S., Shalygin, A., Gudermann, T., Chubanov, V., & Dietrich, A. (2024). TRPM2 channels are essential for regulation of cytokine production in lung interstitial macrophages. *Journal of Cellular Physiology*, 239, e31322. <https://doi.org/10.1002/jcp.31322>